



Enhanced Design of Piston Cooling Nozzles via Computational Fluid Dynamics



Xianren Zeng^{1,2,3*}, Jiahui Zhang², Linmei Li¹, Jiexiang Zuo³

¹ School of Intelligent Manufacturing, Hunan University of Science and Engineering, 425199 Yongzhou, China

² School of Mechanical and Intelligent Manufacturing, Jiujiang University, 332005 Jiujiang, China

³ Jiujiang Huirui Machinery Co., Ltd., 332000 Jiujiang, China

* Correspondence: Xianren Zeng (waclin@huse.edu.cn)

Received: 02-13-2024

Revised: 03-17-2024

Accepted: 03-24-2024

Citation: X. R. Zeng, J. H. Zhang, L. M. Li, and J. X. Zuo, "Enhanced design of piston cooling nozzles via computational fluid dynamics," *Power Eng. Eng. Thermophys.*, vol. 3, no. 1, pp. 45–57, 2024. <https://doi.org/10.56578/peet030104>.



© 2024 by the author(s). Published by Acadlore Publishing Services Limited, Hong Kong. This article is available for free download and can be reused and cited, provided that the original published version is credited, under the CC BY 4.0 license.

Abstract: To elucidate the relationship between the flow rate of an engine's piston cooling nozzle and its internal structure, a structural model of the piston cooling nozzle and a three-dimensional model of the internal flow field were established through an analysis of the nozzle's structural characteristics and operational conditions. Flow field simulations were conducted using Fluent software, yielding velocity and pressure distribution maps as well as flow rate data within the fluid domain of the piston cooling nozzle. Additionally, the variation in flow rate with changes in the nozzle throat length and diameter was investigated. It was found that the flow rate decreases linearly with an increase in nozzle throat length, while it exhibits a nonlinear increase with an increase in throat diameter. Compared to changes in throat length, modifications in throat diameter have a more significant impact on the flow rate of the piston cooling nozzle. An analytical expression for the flow rate as a function of throat diameter was also derived, providing valuable insights and guidance for the engineering design of nozzles.

Keywords: Piston cooling nozzle; Flow field analysis; Numerical simulation; Data fitting

1 Introduction

Turbine supercharging technology significantly enhances engine power while concurrently increasing the thermal load of the engine. Ensuring the piston operates normally under high-temperature conditions necessitates a focus on cooling measures [1]. During engine operation, high-speed reciprocating movements of the piston along the cylinder axis introduce elevated temperatures to the piston head, necessitating cooling measures to maintain piston performance [2]. Failure of the cooling nozzle can precipitate a sharp rise in the operating temperature of the piston, leading to cylinder scoring and potentially rendering the entire engine inoperative [3]. Therefore, cooling of the piston head is critical, with prevalent methods including free nozzle cooling, oscillatory cooling, and forced oscillatory cooling through internal oil channels [4].

The study of cooling internal combustion engine cylinders and components has a long history. Nasif et al. [5] employed an Improved Delayed Detached Eddy Simulation (IDDES) to address the thermal-fluid coupling challenges beneath the exhaust valve. Renso et al. [6] optimized the piston temperature field using a genetic algorithm and estimated the heat transfer coefficients in the piston area, providing technical support for piston cooling. The implementation of jet cooling techniques for the piston is crucial, with El-Khawankey et al. [7] investigating the behavior of impinging oil jets on flat walls to identify and assess the parameters affecting oil film formation. Goyal and Agarwal [8] conducted both experimental and numerical studies on the impact jet cooling of flat plates to control non-exhaust emissions in heavy diesel engines, obtaining heat transfer coefficients at the piston bottom. Besides flat plate jet cooling, large eddy simulation methods have also been used to study the cooling performance of cylindrical jets [9].

In addition to jet techniques, numerous studies on the cooling and heat dissipation effects of nozzles have been conducted both domestically and internationally [10], achieving a series of results. Nasif et al. [11] conducted numerical simulations using the finite volume method on the convective heat transfer of impinging jets during the piston cooling process, demonstrating that cooling jets significantly reduce piston temperatures. Agarwal et al. [12]

explored the heat conduction from piston cooling nozzles to the piston through numerical simulations, predicting the heat dissipation coefficients on the underside of the piston and studying the impact of variations in oil injection speed, oil type, nozzle diameter, and the distance between the nozzle and piston on cooling effectiveness. Furthermore, experimental research on the cooling performance of piston cooling nozzles has been undertaken by Easter et al. [13] and Liu et al. [14], who established a regionally averaged heat transfer correlation, specifically the Nusselt number, which showed strong dependence on nozzle diameter and oil viscosity, and weak dependence on the distance from the nozzle to the wall.

Substantial research has been devoted to the application of nozzles in various fields beyond cooling, including fuel injection [15] and thermosyphons [16]. Kawaguchi et al. [17] conducted a detailed study on the external flow field fluctuations of nozzle jets, attributing these fluctuations to those within the nozzle's internal flow field. However, since the heat from the piston is removed by the cooling oil ejected by the nozzle, the nozzle's flow rate is crucial for effective piston cooling. Cao et al. [18] studied the heat transfer characteristics of oscillatory flow in open internal oil chambers of pistons, noting that the nozzle flow rate must neither be too high nor too low. A flow rate too low fails to achieve cooling, whereas too high a rate reduces the engine's thermal efficiency and increases the piston's thermal stress. Kawaguchi et al. [19] examined the impact of different curvature radii of circular 90-degree bend nozzles on the flow rate of piston cooling nozzles. Deng et al. [20] investigated the internal flow field of piston cooling nozzles, obtaining trends in flow rate changes relative to inlet length and internal bore diameter of the nozzle. However, they did not provide a quantitative relationship between these variables, which remains unclear for engineering nozzle design.

Due to the compact internal layout of engines, including piston travel requirements, there is limited scope for altering the overall external structure of piston cooling nozzles. Typically, modifications to throat length and nozzle diameter are made to adjust the ejection flow rate while keeping the total flow path length constant. Thus, in the structural design of piston cooling nozzles, the relationship between nozzle throat length and diameter and nozzle flow rate becomes particularly significant.

This study focuses on the internal flow characteristics and flow rate control of piston cooling nozzles. A model of the internal flow field of a specific engine's piston cooling nozzle was developed, and its jet flow rate was studied through experimental and simulation comparisons to establish a simulation flow field model that aligns with engineering practices. Based on this, simulation experiments were conducted on the simulation flow field model to explore the variation in nozzle flow rate with different throat lengths and diameters, under the condition of constant total flow path length.

Innovation and significance of this study: By employing polynomial fitting, a theoretical solution for the nozzle flow rate in relation to the throat diameter was proposed, offering practical value for the engineering design of piston cooling nozzles.

2 Experiments and Methods

2.1 Research Methods

The Finite Element Method (FEM) is commonly employed to solve flow field problems. In the fluid domain of the nozzle, all fluid particles adhere to the three fundamental equations of fluid mechanics:

$$\begin{aligned} \frac{\partial \rho}{\partial t} + \text{div}(\rho \vec{v}) &= 0 \\ \frac{\partial \vec{v}}{\partial t} + (\vec{v} \cdot \nabla) \vec{v} &= \vec{F} - \frac{1}{\rho} \nabla p + \nu \Delta \vec{v} \\ \frac{D}{Dt} \left(\frac{1}{2} u_i u_i \right) &= u_i F_{x_i} + \frac{1}{\rho} u_i \frac{\partial p_{ij}}{\partial x_j} \end{aligned} \quad (1)$$

where, ρ represents the density, \vec{v} denotes the velocity vector of the fluid particle, u_i represents the velocity component of the fluid particle, \vec{F} denotes the body force, p represents the surface force, and ν denotes the kinematic viscosity of the fluid. By simultaneously solving these three fundamental equations, the velocity distribution, pressure distribution, and flow rate within the piston cooling nozzle's fluid domain can be obtained.

With the rapid advancement of computer technology, the internal flow field of the piston cooling nozzle can be calculated using the FEM and integrated within the Fluent software.

Furthermore, the piston cooling nozzle was mounted on a target test bench to measure the flow rate ejected under different oil pressures. Concurrently, the kinematic viscosity, density, and other physical parameters of the oil used in the tests were determined. A three-dimensional model of the piston cooling nozzle structure was then developed, from which the flow field model of the piston cooling nozzle was extracted. Based on fundamental Computational Fluid Dynamics (CFD) principles and boundary conditions consistent with experimental tests, the internal flow field within the piston cooling nozzle was solved to ultimately ascertain the theoretical flow rate. This theoretical flow rate was compared with empirical results to refine simulation parameters, ensuring a high degree of agreement between simulation outputs and experimental outcomes, thereby substituting physical experiments for further research.

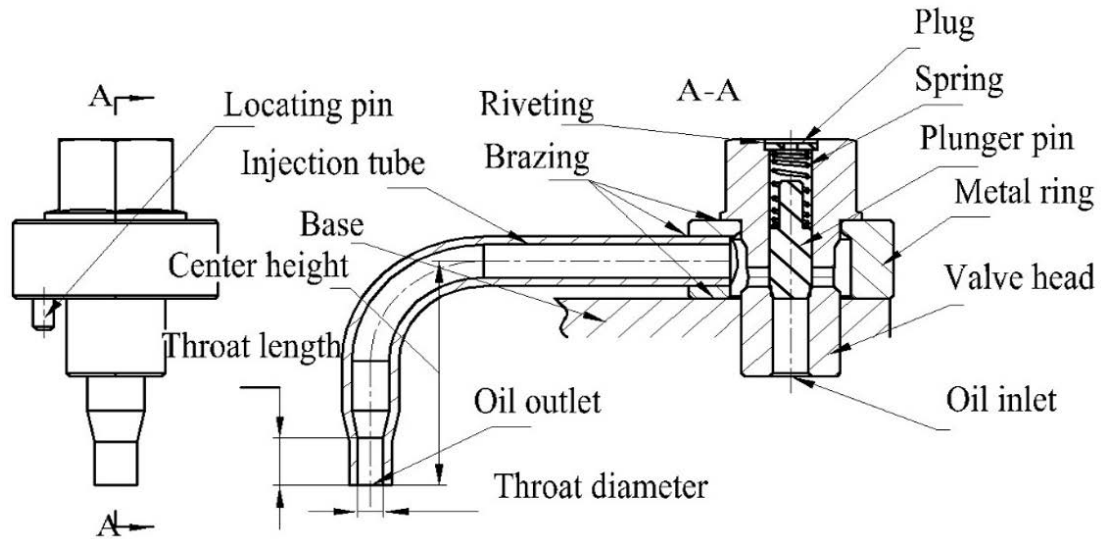


Figure 1. Structural diagram of the piston cooling nozzle

Due to the compact nature of engine structures, the installation location and space for piston cooling nozzles are restricted. Thus, while the overall geometric parameters remain largely unchanged, design modifications to the nozzle structure primarily consider the nozzle's throat length and diameter. The throat length refers to the length of the contracted part of the spray tube at the outlet, as clearly indicated in Figure 1. Finally, through simulation experiments in the optimized computational model within Fluent software, adjustments to the nozzle outlet diameter and throat length were made to study the variation in flow rates with different nozzle structures.

2.2 Physical Experiments

Initially, the cooling oil was formulated by purchasing motor oil and diluent, repeatedly adjusting the mixture ratio to achieve a viscosity of 10.5 cst (mm^2/s) for experimental testing. The viscosity of the cooling oil was measured using a BCYD-800 kinematic viscometer. Figure 2 illustrates the BCYD-800 viscometer being used for the viscosity testing experiment.



Figure 2. Viscosity testing experiment

The prepared cooling oil was then introduced into the piston cooling nozzle at the target testing bench. A targeting experiment was conducted with the piston cooling nozzle, yielding parameters such as pressure and flow rate. Figure 3 shows the dimensions of the internal flow paths of the tested nozzle. Based on Figure 3, ten nozzles were produced and subjected to targeting experiments. The flow rates of the tested nozzles are displayed in Table 1. After several testing experiments, at an inlet oil pressure of 400 kPa, the average flow rate of the piston cooling nozzle was determined to be 12.3 L/min. Figure 4 depicts the experimental setup of the piston cooling nozzle.

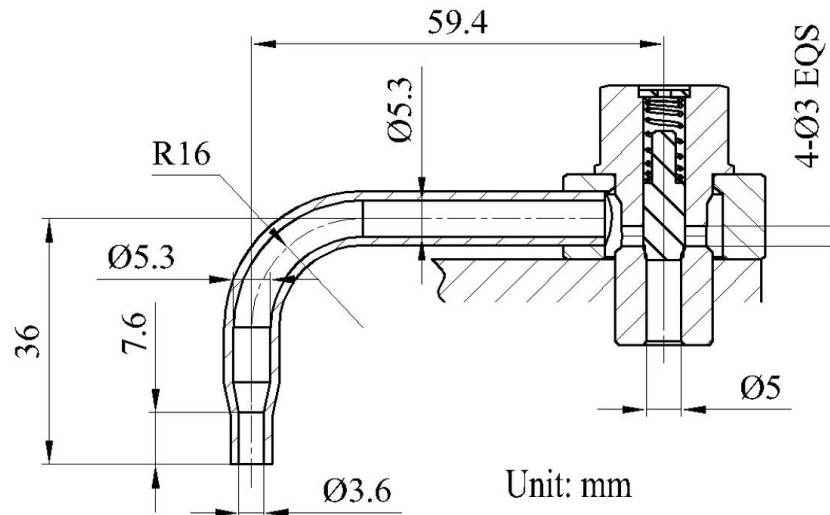


Figure 3. Dimensional diagram of the tested nozzle

Table 1. Flow rates of tested nozzles

No.	1 #	2 #	3 #	4 #	5 #	6 #	7 #	8 #	9 #	10 #
Flow Rate (L/min)	12.2	12.14	12.3	12.18	12.49	12.52	12.34	12.28	12.17	12.3

2.3 Simulation Study

Initially, a three-dimensional model was established based on the dimensions of the piston cooling nozzle shown in Figure 3. Subsequently, the three-dimensional model of the flow field domain within its internal cavity was extracted.

2.3.1 Three-dimensional modeling of the piston cooling nozzle

The primary function of the piston cooling nozzle is to inject engine oil accurately and quantitatively into the cooling oil chamber at the top of the engine piston, thereby achieving the objective of cooling the engine piston. The piston cooling nozzle is typically installed at the end of the engine cylinder. The installation positions are marked with yellow frames in Figure 5.

The piston cooling nozzle mainly consists of a valve head, injection tube, locating pin, plug, plunger, and spring. Figure 1 provides a simplified structural diagram. From this diagram, it can be observed that when the cooling oil enters through the inlet, it pushes the plunger upward, compressing the spring. Subsequently, the cooling oil enters the injection tube and is expelled through the outlet, cooling the engine piston.

2.3.2 Flow field modeling of the piston cooling nozzle

In order to investigate the state and properties of fluid flow within the piston cooling nozzle, a three-dimensional model of the fluid domain is required. Initially, the nozzle structure was digitally modeled in three dimensions using SolidWorks software. Subsequently, the external surface of the nozzle model was extracted, and both the oil inlet and outlet were sealed and filled to create a solid model of the piston cooling nozzle. By performing a Boolean subtraction of the solid nozzle model from the original nozzle model, the fluid domain model of the piston cooling nozzle was obtained, as shown in Figure 6.

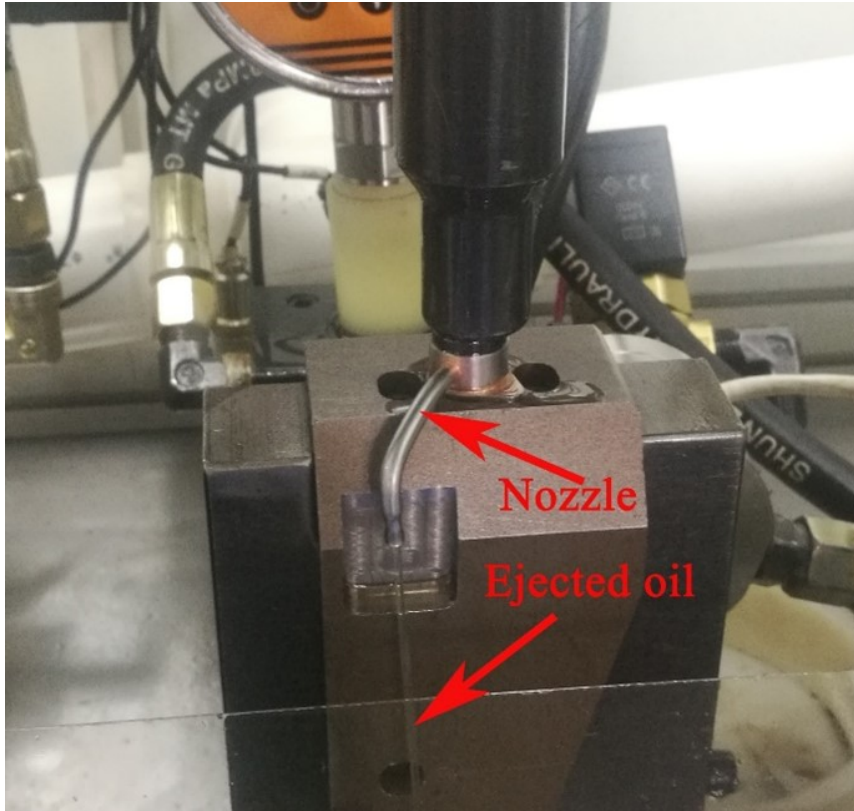


Figure 4. Experimental setup of the piston cooling nozzle

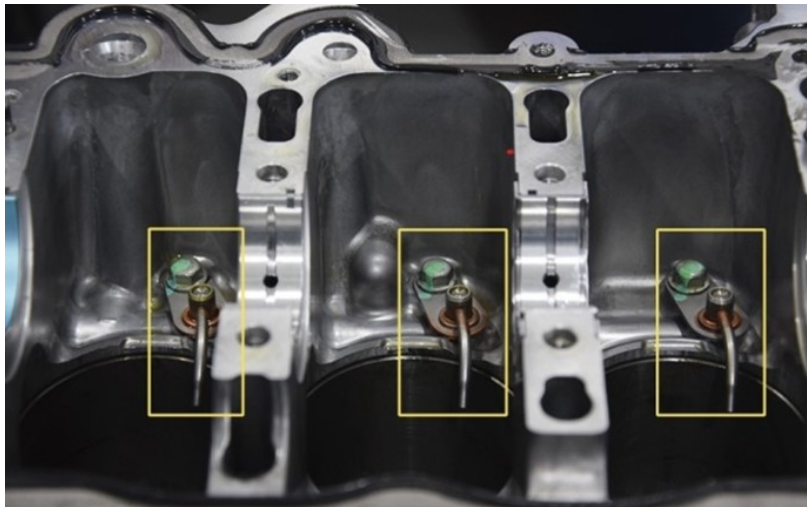


Figure 5. Installation positions of the nozzles

2.3.3 Mesh generation

For solving the fluid domain using the FEM, it is essential to discretize the internal flow field of the piston cooling nozzle into numerous small elements. A coarse mesh with fewer elements reduces computational load but lacks precision. Conversely, a fine mesh increases the number of elements, enhancing accuracy but requiring more time and higher computational resources. Therefore, the mesh is designed to minimize the number of elements while satisfying the required accuracy. The mesh generation should adhere to the following principles: (i) The number of mesh nodes should be maximized to obtain more accurate results. (ii) The maximum and minimum sizes of the mesh should not vary excessively, ideally remaining within a ratio of 1.2 to 1.4. (iii) Element nodes should connect directly to neighboring element nodes and not be positioned on adjacent boundaries. (iv) The mesh should be fixed as much as possible to facilitate automatic generation by the computer.

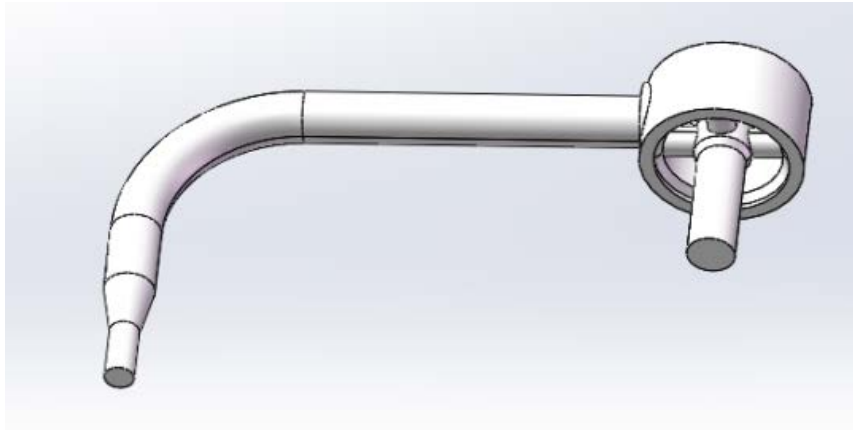


Figure 6. Fluid domain model of the piston cooling nozzle

In this study, an automatic meshing tool was employed for mesh generation, with operations as follows: First, the inlet, outlet, and boundaries were defined and named. Considering that the fluid velocity adheres to zero at the wall and is higher towards the center, resulting in a velocity gradient, a boundary layer setting was applied. An additional five layers of refined annular meshes were added near the inner surface of the piston cooling nozzle to densify the boundary layer mesh relative to other areas, accommodating the computational precision required by significant velocity gradients. Figure 7 depicts the mesh model generated. The overall mesh quality was evaluated for skewness and orthogonality, ensuring that the mesh quality was sufficiently high to guarantee steady convergence of the model solution.

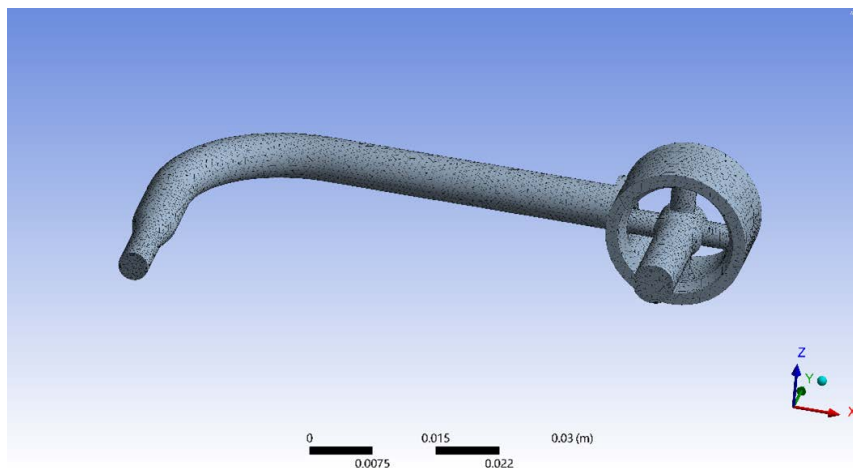


Figure 7. Fluid mesh of the piston cooling nozzle

2.3.4 Determination of boundary conditions

Based on the actual operating conditions of the piston cooling nozzle, the inlet oil pressure was set at 400 kPa, with the outlet open to the atmosphere, defined as standard atmospheric pressure. Accordingly, within the mesh, the inlet, outlet, and wall surfaces were named. The mesh was imported into Fluent, and the parameters were set under “Boundary Conditions” in Fluent as follows: the wall was defined with default settings as a no-slip, smooth solid wall.

2.3.5 Properties of the fluid material

The fluid primarily used for engine piston cooling is engine oil with a viscosity of 10.5 cst. Therefore, the density of the fluid material was set at 910 kg/m^3 , with a corresponding kinematic viscosity of $0.009555 \text{ Pa}\cdot\text{s}$.

2.3.6 Flow field solution

Fluent offers three fundamental methods for solving flow fields: coupled implicit, coupled explicit, and uncoupled solutions. The uncoupled solution is generally used for incompressible or low Mach number compressible fluid flows. Given that this study only involves the internal flow field, an uncoupled solution was selected. Additionally, Fluent

provides a variety of computational models. After comparing many of these models with physical experiments, the optimal computational model was chosen.

The solution of linear equations typically utilizes the relaxation iteration method, which includes relaxation factors to regulate the convergence speed of the equations. The relaxation factors for various parameters are shown in Table 2. The convergence residuals for each parameter are presented in Table 3. Turbulence intensity and the viscosity ratio at the nozzle inlet were set at 5% and 10, respectively, while the outlet backflow turbulence intensity and viscosity ratio were also set at 5% and 10.

Table 2. Relaxation factors for various parameters

Parameter	Pressure	Density	Body Force	Momentum	Turbulent Kinetic Energy	Turbulent Dissipation Rate	Turbulent Viscosity
Relaxation Factor	0.3	1	1	0.1	0.8	0.8	1

Table 3. Convergence residuals for parameters

Parameter	Continuity	x-velocity	y-velocity	z-velocity	k	Epsilon
Residual	0.001	0.001	0.001	0.001	0.001	0.001

In Fluent, the Semi-Implicit Method for Pressure-Linked Equations (SIMPLE) algorithm was employed for numerical solution. Pressure and momentum were solved using a second-order upwind scheme, while turbulent kinetic energy and turbulent dissipation rate were solved using a first-order upwind scheme. Standard initialization was chosen, with each parameter initialized at zero. The computational program commenced from the nozzle inlet. The maximum number of iterations was set at 1000.

3 Results and Discussion

Table 4. Nozzle flow rates under different computational models

Computational Model	Fluent Simulation Results							Physical Experiment Results
	Laminar	Spalart-Allmaras	k-epsilon Standard with Spalart-Allmaras	k-omega Wundard Wunction	Transition k-k1-Standard	Transition SST	Reynolds Stress	
Flow Rate (L/min)	13.05	12.92	12.51	12.9	12.73	12.92	12.76	12.3

A variety of computational models were employed to solve the flow field of the piston cooling nozzle under identical boundary conditions. Table 4 presents the nozzle flow rates derived from different computational models and physical experiments. The Laminar model, primarily applied to calculations within the laminar flow domain, is one example. The Spalart-Allmaras model, a low Reynolds number model developed for aerodynamic flows, has not been calibrated for general industrial flows and indeed produces relatively significant errors in certain free shear flows, particularly in plane and circular jets. The k-epsilon model, based on the Reynolds-averaged assumption, decomposes turbulence into macroscopic mean flow and turbulent fluctuations, simulating turbulent behavior through the calculation of energy and momentum equations. This model is suited for scenarios with high turbulence intensity, such as within boundary layers and at free surfaces. The standard k-omega model is an empirical model based on the transport equations for turbulence kinetic energy (k) and specific dissipation rate (ω), which can also be considered as the ratio of ω to k. This model includes adjustments for low Reynolds number effects, compressibility, and shear flow spreading. Over the years, modifications to the model have added production terms to the transport equations for turbulence kinetic energy and specific dissipation rate, enhancing the model's accuracy in predicting free shear flows. The Transition k-kl-omega is a three-equation transition model, used to simulate the transition from laminar to turbulent flow. The Transition SST is a four-equation transition model, used for simulating the turbulence transition process, providing better accuracy and stability in the near-wall region compared to the standard k-omega model. The Reynolds stress model is a seven-equation model, not assuming isotropy like other RANS models, thus making it suitable for strong swirling flows.

Due to the high viscosity of the engine oil ejected by the piston cooling nozzle, the internal flow within the nozzle is relatively stable, with limited turbulent vortex states. Hence, the standard k-epsilon model was deemed appropriate. As shown in Table 4, the simulation results from the standard k-epsilon model are the closest to the experimental data. Figure 8 displays the velocity cloud diagram for the internal flow field of the piston cooling nozzle under the k-epsilon standard model. Upon the oil's initial entry into the nozzle, this segment is in a transitional state, maintaining a minimal and stable velocity, indicative of a turbulent state. As the fluid moves further into the downstream pipe, it remains relatively stable, though there are indications of acceleration in the latter part of the pipe. Upon passing through the nozzle's constriction, a sudden change in velocity occurs, reaching its maximum at the outlet while maintaining a laminar flow state, ensuring that nearly all the oil is directed onto the piston. The simulation results under the standard k-epsilon model indicate a nozzle flow rate of 0.1898 kg/s, which converts to 12.51 L/min.

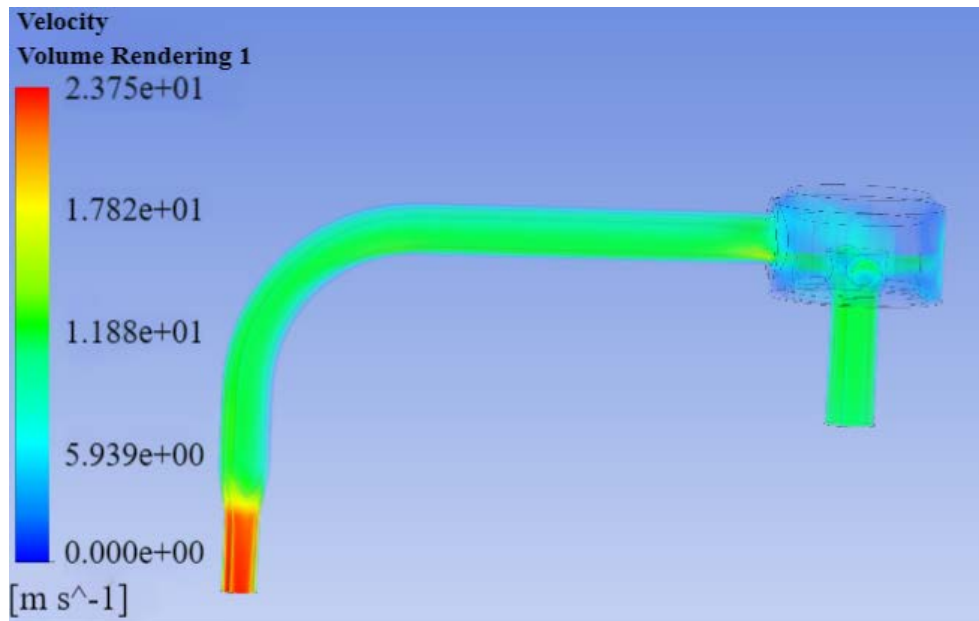


Figure 8. Velocity cloud diagram in the nozzle under the k-epsilon model

For different engines, the thermal dissipation power varies. Therefore, the flow rate requirements for the piston cooling nozzle also differ. Typically, the nozzle outlet is modified to change the shape and size of the piston cooling nozzle outlet, achieving various ejection flow rates.

3.1 Impact of Throat Length on Flow Rate of the Piston Cooling Nozzle

Using the nozzle depicted in Figure 3 as the model, with a throat diameter of 3.6 mm, the effect of changes in throat length from 0 to 15 mm on nozzle flow rate was investigated. The same boundary conditions as described in Section 1.3 were applied, and Fluent software was used to calculate 16 data points for throat lengths ranging from 0 to 15 mm. Table 5 presents the calculated results.

Table 5. Flow rate data of the piston cooling nozzle at different throat lengths

Throat Length (mm)	0	1	2	3	4	5	6	7
Mass Flow Rate (kg/s)	0.197	0.1945	0.1931	0.1917	0.1908	0.1896	0.1885	0.1875
Volumetric Flow Rate (L/s)	0.216	0.213	0.212	0.211	0.209	0.208	0.207	0.206
Throat Length (mm)	8	9	10	11	12	13	14	15
Mass Flow Rate (kg/s)	0.1867	0.1857	0.185	0.184	0.1831	0.1821	0.1813	0.1806
Volumetric Flow Rate (L/s)	0.205	0.204	0.203	0.202	0.201	0.2	0.199	0.198

To visually depict the trend of nozzle flow rate in response to changes in throat length, the volumetric flow rates from Figure 6 were plotted as a curve, as shown in Figure 9. The curve illustrates that as the throat length increases, the nozzle flow rate exhibits a decreasing trend, with a rapid decline initially followed by a slower decrease, overall showing a linear change.

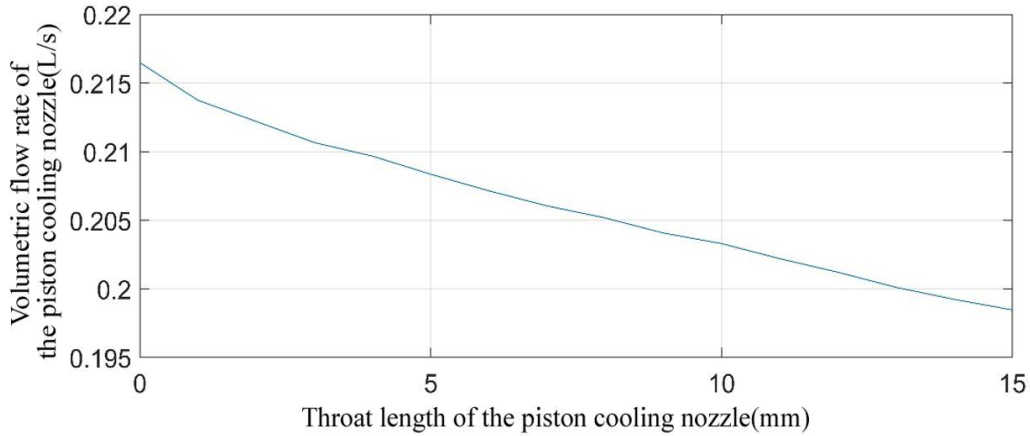


Figure 9. Flow rate curve of the piston cooling nozzle changing with throat length

3.2 Impact of Throat Diameter on Flow Rate of the Piston Cooling Nozzle

In addition to throat length, the throat diameter also significantly influences the flow rate of the nozzle. Under unchanged conditions, modifications were made to the throat diameter of the piston cooling nozzle. Using Fluent software, the flow rates of nozzles with various throat diameters were calculated. Figure 10 illustrates the flow rate curve of the piston cooling nozzle under different throat diameters. It is observed from the graph that as the throat diameter increases, the flow rate of the nozzle exhibits a rising trend, with changes displaying a distinct non-linearity.

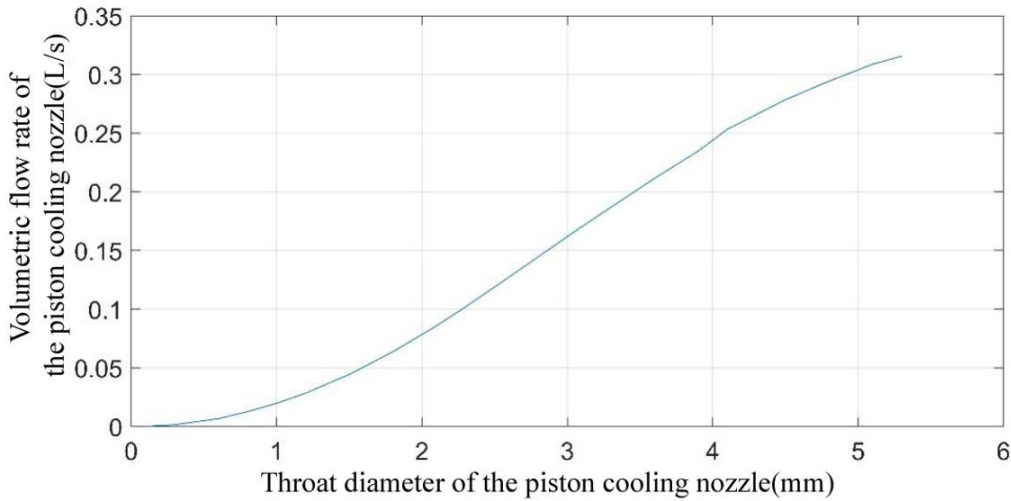


Figure 10. Flow rate curve of the piston cooling nozzle changing with throat diameter

By comparing Figure 9 and Figure 10, it can be observed that changes in throat diameter have a more significant impact on flow rate compared to changes in throat length. To enhance the application in engineering projects, polynomial fitting was performed on the simulation data from Figure 10. Figure 11 presents the quadratic polynomial fitting curve, while Figure 12 shows the cubic polynomial fitting curve.

From the figures above, it is evident that the simulation data of the flow rate and the throat diameter of the piston cooling nozzle align very closely with the cubic polynomial fitting curve. The following analytical expression was derived:

$$Q = -0.0036d^3 + 0.0327d^2 - 0.0126d + 0.0023 \quad (2)$$

where, Q represents the flow rate (L/s), and d denotes the throat diameter (mm).

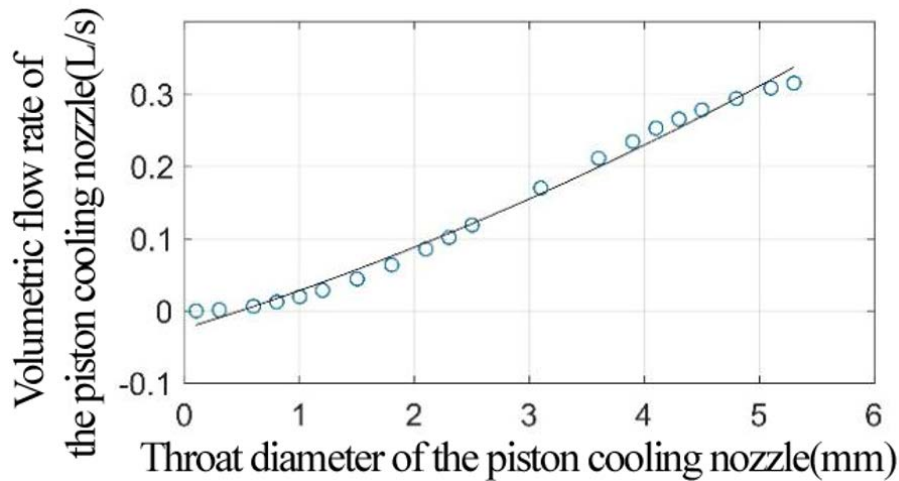


Figure 11. Quadratic polynomial fitting curve for flow rate of the piston cooling nozzle

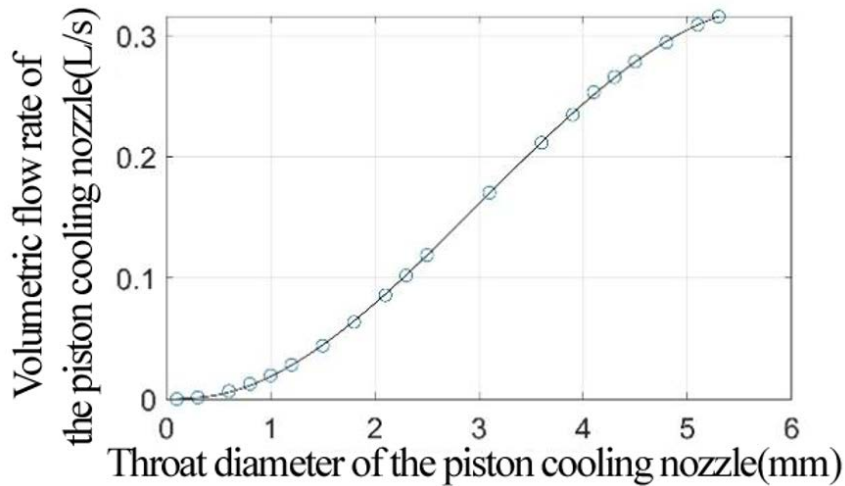


Figure 12. Cubic polynomial fitting curve for flow rate of the piston cooling nozzle

3.3 Comparative Experimental Study

To verify the accuracy of Eq. (2), experimental tests were conducted on nozzles with various throat diameters. More than ten piston cooling nozzles with throat diameters of 1.2mm, 2mm, 3mm, 4mm, and 5mm were fabricated. Using 10.5cst engine oil, targeting experiments were carried out at an inlet pressure of 400kPa. For each type of nozzle, targeting tests were performed on ten samples, and the average flow rate was recorded as the composite flow rate for that nozzle, as shown in Table 6. Figure 13 displays the processed experimental nozzle samples.

Table 6. Flow rate test table for nozzles with different throat diameters (L/s)

Throat Diameter mm	No.										Average
	1 #	2 #	3 #	4 #	5 #	6 #	7 #	8 #	9 #	10 #	
∅1.2	0.024	0.026	0.027	0.024	0.026	0.027	0.027	0.027	0.024	0.020	0.025
∅2	0.058	0.058	0.055	0.059	0.059	0.057	0.058	0.055	0.057	0.071	0.058
∅3	0.169	0.163	0.165	0.171	0.166	0.164	0.170	0.163	0.163	0.172	0.166
∅4	0.231	0.231	0.236	0.232	0.230	0.231	0.232	0.236	0.234	0.240	0.233
∅5	0.301	0.297	0.302	0.298	0.297	0.302	0.298	0.297	0.301	0.356	0.3

The experimental data and the theoretical values from Eq. (2) were compared, as displayed in Table 7. It is evident that both the theoretical and experimental values of nozzle flow rate increase with the increase in throat diameter.



Figure 13. Processed and tested experimental nozzle samples

Table 7. Comparative analysis of experimental tests and theoretical calculations for nozzle flow rates at different throat diameters

Throat Diameter (mm)	Ø1.2	Ø2	Ø3	Ø4	Ø5
Theoretical Value of Eq. (2) (L/s)	0.028	0.0791	0.1616	0.2447	0.3068
Experimental Value (L/s)	0.025	0.058	0.166	0.233	0.3

To provide a more visual comparison of theoretical calculations and actual data, the data from Table 6 were plotted, resulting in a graph showing the comparison of theoretical and actual flow rates of nozzles with different throat diameters (Figure 14). The graph reveals a good alignment between the predicted values and experimental outcomes. Variations in data points, both large and small, suggest the presence of some experimental errors.

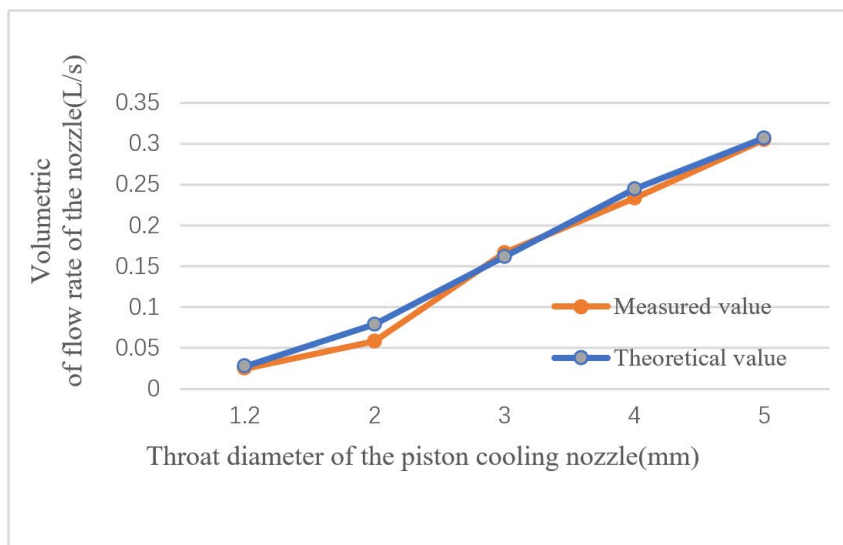


Figure 14. Comparison of theoretical and experimental flow rates for piston cooling nozzles with different throat diameters

3.4 Analysis and Discussion

The results of the study indicate that with a 15mm extension in the throat length of the piston cooling nozzle, the flow rate decreases by only about 0.015 L/s. This suggests that the per-unit-length loss in pipe flow is relatively small. However, when the throat diameter increases from 1.2 mm by about 4 mm, the nozzle flow rate increases by approximately 0.3 L/s. It is evident that changes in nozzle diameter have a significant impact on the flow rate of the piston cooling nozzle, primarily because fluid flows in the pipe, with the highest velocity in the central area and zero velocity in the boundary layer. Due to the thinness of the boundary layer, when the diameter increases, a substantial amount of boundary layer fluid enters the central free area, attaining a higher velocity, thereby increasing the flow rate.

4 Conclusions

In this study, a three-dimensional model of the piston cooling nozzle was developed, along with a three-dimensional model of its internal fluid domain. The actual operating conditions of the piston cooling nozzle were analyzed to establish its working boundary conditions. Utilizing the CFD solving capabilities of Fluent software, the internal flow of the piston cooling nozzle under actual operating conditions was simulated, yielding the theoretical ejection flow rate of the nozzle. Experimental testing validated and confirmed the computational model that corresponds with the actual operating conditions of the piston cooling nozzle. Subsequently, this model was employed to investigate the impact of changes in the nozzle's throat length from 0 mm to 15 mm and the changes in throat diameter from 0.1 mm to 5.3 mm on the flow rate of the piston cooling nozzle. The results indicate that, with other conditions held constant, as the nozzle throat length gradually increased from 0 to 15 mm, the flow rate of the piston cooling nozzle decreased from 216 mL/s to 198 mL/s. However, with other boundary conditions fixed, solely increasing the throat diameter from 0.1 mm to 5.3 mm caused the flow rate of the piston cooling nozzle to rapidly increase from 0.083 mL/s to 315.6 mL/s. To more clearly articulate the variation in flow rate with changes in nozzle diameter, polynomial fitting methods were utilized along with experimental verification to establish that the flow rate of the piston cooling nozzle is a cubic polynomial function of the nozzle diameter.

Further studies could be conducted on the flow rate curves of the piston cooling nozzle under various inlet pressure conditions, thereby plotting isobaric flow rate curves for different throat diameters to facilitate nozzle engineering design.

Funding

This project received funding from the Key Research and Development Plan of the Science and Technology Department of Jiangxi Province (Grant No.: 20203BBE52W017) and the Science and Technology Project of the Education Department of Jiangxi Province (Grant No.: GJJ201811).

Data Availability

The data used to support the findings of this study are available from the corresponding author upon request.

Conflicts of Interest

The authors declare no conflict of interest.

References

- [1] O. Nilaphai, K. Komane, and S. Chuepeng, "Expansion heat release and thermal efficiency of acetone-butanol-ethanol-diesel blended fuel (ABE20) combustion in piston engine," *Fuel*, vol. 309, p. 122214, 2022. <https://doi.org/10.1016/j.fuel.2021.122214>
- [2] X. Deng, H. Chen, J. Lei, D. Jia, and Y. Bi, "Controllable thermal state design method of flexible shapes of piston cooling galleries," *Appl. Therm. Eng.*, vol. 191, p. 116865, 2021. <https://doi.org/10.1016/j.applthermaleng.2021.116865>
- [3] M. O. Tas, A. Banerji, M. Lou, M. J. Lukitsch, and A. T. Alpas, "Roles of mirror-like surface finish and DLC coated piston rings on increasing scuffing resistance of cast iron cylinder liners," *Wear*, vol. 376, pp. 1558–1569, 2017. <https://doi.org/10.1016/j.wear.2017.01.110>
- [4] X. Yu, D. Yi, Y. Huang, Y. Lu, and A. P. Roskilly, "Experimental investigation of two-phase flow and heat transfer performance in a cooling gallery under forced oscillation," *Int. J. Heat Mass Transf.*, vol. 132, pp. 1306–1318, 2019. <https://doi.org/10.1016/j.ijheatmasstransfer.2018.12.089>
- [5] G. Nasif, A. M. Shinneeb, and R. Balachandar, "Cooling enhancement for engine parts using jet impingement," *Front. Mech. Eng.*, vol. 10, p. 1251587, 2024. <https://doi.org/10.3389/fmech.2024.1251587>
- [6] F. Renso, M. Giacomini, S. G. Barbieri, and V. Mangeruga, "Oil jets piston cooling: A numerical methodology for the estimation of heat transfer coefficients and optimization of the piston temperature field through a genetic algorithm," *Proc. Inst. Mech. Eng. D J. Automob. Eng.*, 2023. <https://doi.org/10.1177/09544070231161909>
- [7] S. El-Khawankey, F. Al-Sibai, and R. Kneer, "Impinging oil jet behaviour for planar wall heat transfer," in *International Heat Transfer Conference, Napoli, Italy*, 2010, pp. 639–645. <https://doi.org/10.1115/IHTC14-22805>
- [8] S. K. Goyal and A. K. Agarwal, "Experimental and numerical investigations of jet impingement cooling of flat plate for controlling the non-tail pipe emissions from heavy duty diesel engines," in *Internal Combustion Engine Division Spring Technical Conference, Aachen, Germany*, vol. 42061, 2006, pp. 179–186. <https://doi.org/10.1115/ICES2006-1434>

- [9] S. S. Moghe and S. M. Janowiak, "Large eddy simulation of cylindrical jet breakup and correlation of simulation results with experimental data," *J. Eng. Gas Turbines Power*, vol. 139, no. 10, p. 102811, 2017. <https://doi.org/10.1115/1.4036528>
- [10] A. Jacob, K. A. Shafi, and K. E. Reby Roy, "Enhancement of heat transfer in a synthetic jet actuated by piston cylinder," *Adv. Mech. Eng.*, vol. 13, no. 9, 2021. <https://doi.org/10.1177/16878140211049139>
- [11] G. Nasif, R. M. Barron, and R. Balachandar, "Numerical simulation of piston cooling with oil jet impingement," *J. Heat Transf.*, vol. 138, no. 12, p. 122201, 2016. <https://doi.org/10.1115/1.4034162>
- [12] A. K. Agarwal, S. K. Goyal, and D. K. Srivastava, "Time resolved numerical modeling of oil jet cooling of a medium duty diesel engine piston," *Int. Commun. Heat Mass Transf.*, vol. 38, no. 8, pp. 1080–1085, 2011. <https://doi.org/10.1016/j.icheatmasstransfer.2011.05.006>
- [13] J. Easter, C. Jarrett, C. Pespisa, Y. C. Liu, A. C. Alkidas, L. Guessous, and B. P. Sangeorzan, "An area-average correlation for oil-jet cooling of automotive pistons," *J. Heat Transf.*, vol. 136, no. 12, p. 124501, 2014. <https://doi.org/10.1115/1.4027835>
- [14] Y. C. Liu, L. Guessous, B. P. Sangeorzan, and A. C. Alkidas, "Laboratory experiments on oil-jet cooling of internal combustion engine pistons: Area-average correlation of oil-jet impingement heat transfer," *J. Energy Eng.*, vol. 141, no. 2, 2015. [https://doi.org/10.1061/\(ASCE\)EY.1943-7897.0000227](https://doi.org/10.1061/(ASCE)EY.1943-7897.0000227)
- [15] J. Eismark, M. Christensen, M. Andersson, A. Karlsson, and I. Denbratt, "Role of fuel properties and piston shape in influencing soot oxidation in heavy-duty low swirl diesel engine combustion," *Fuel*, vol. 254, p. 115568, 2019. <https://doi.org/10.1016/j.fuel.2019.05.151>
- [16] S. W. Chang and K. C. Yu, "Thermal performance of reciprocating two-phase thermosyphon with nozzle," *Int. J. Therm. Sci.*, vol. 129, pp. 14–28, 2018. <https://doi.org/10.1016/j.ijthermalsci.2018.02.032>
- [17] M. Kawaguchi, R. Nakayama, L. Ma, K. Nishida, H. Yokohata, M. Koutoku, J. Nishikawa, A. Nakashima, and Y. Ogata, "Effects of characteristic decomposed modes of the internal flow of a circular 90-degree bent nozzle on the behavior of the oil jet interface," *J. Fluid Sci. Technol.*, vol. 16, no. 4, p. JFST0023, 2021. <https://doi.org/10.1299/jfst.2021jfst0023>
- [18] Y. Cao, W. Zhang, Z. Yang, Y. Yuan, and H. Zhu, "An investigation into the flow and heat transfer characteristics of an open cooling gallery in piston," *Automo Eng*, vol. 36, no. 5, pp. 546–551, 2014.
- [19] M. Kawaguchi, G. Nitta, K. Mimura, K. Nishida, M. Koutoku, R. Yamamoto, A. Nakashima, and Y. Ogata, "Effect of flow in the circular 90-degree curved nozzles on ejecting oil jet behavior," *J. Fluid Sci. Technol.*, vol. 16, no. 2, p. JFST0011, 2021. <https://doi.org/10.1299/jfst.2021jfst0011>
- [20] L. J. Deng, Z. M. Wang, and Y. Q. Liu, "Effect of structural parameters on fill ratio of closed cooling gallery," *J Cent South Univ (Sci Tech)*, vol. 48, no. 8, pp. 2224–2230, 2017.